British Journal of Pharmacology (1998) 125, 741–750 
http://www.stockton-press.co.uk/bjp

# Use-dependent block of $I_h$ in mouse dorsal root ganglion neurons by sinus node inhibitors

[1,3]A. Raes, [1,2]G. Van de Vijver, [1]M. Goethals & [1]P.P. van Bogaert

[1]Laboratory for Electrophysiology, Department of Biochemistry, Physiology and Genetics, University of Antwerp (RUCA), B-2020 Antwerp, Belgium

**1** The sinus node inhibitors UL–FS 49 and DK–AH 269 reduce heart rate by slowing diastolic depolarization rate in the sino-atrial (SA) node, which might originate from the use-dependent blockade of a hyperpolarization-activated current $I_f$. A hyperpolarization-activated current $I_h$, which is present in many types of neurons, is similar to $I_f$. We studied the effects of these drugs on $I_h$ in cultured mouse dorsal root ganglion (DRG) neurons.

**2** With the whole-cell patch-clamp technique use-dependent block of $I_h$ was observed. The steady-state block following a voltage-clamp pulse train (1-s steps from −38 to −108 mV applied at 0.5 Hz) was dependent on drug concentration and showed an apparent $K_d$ of 0.1 and 0.79 $\mu$M with DK–AH 269 and UL–FS 49 respectively.

**3** The rate of block increased linearly with drug concentration. The rate of recovery from block was, however, much slower compared to cardiac tissue.

**4** There was no significant effect of UL–FS 49 on the activation curve.

**5** At high concentrations of UL–FS 49 a clear association of the drug with the open channel was observed.

**6** When the cell was stimulated at a frequency of 3 Hz, a distinct hyperpolarization was observed in the presence of extracellular $Cs^+$ or when $I_h$ was blocked with UL–FS 49, but not in the absence of $Cs^+$ and UL–FS 49.

**7** These results indicate that $I_h$ protects the cell against hyperpolarizations and subsequent inexcitability. The action of the drugs on the hyperpolarization-activated current in cardiac and neuronal tissue show some similarities; however, some pronounced differences indicate that different subtypes of the channel might exist.

**Keywords:** Sinus node inhibitor; use-dependent block; mouse dorsal root ganglion (DRG) neurons; hyperpolarization-activated current $I_h$; membrane potential

## Introduction

The drugs UL–FS 49 and DK–AH 3 (Figure 1) are derivatives of verapamil that induces changes in distinct electrical properties. The racemic mixture DK–AH 3 consists of a left (DK–AH 269) and right (DK–AH 268) stereo isomer with DK–AH 269 as the more potent one (van Bogaert & Raes, 1993). These sinus node inhibitors, or specific bradycardic agents, form a class of cardiac drugs selectively reducing heart rate by slowing diastolic depolarization rate in the SA node (Kobinger, 1989). As these drugs can reduce myocardial oxygen consumption and increase oxygen supply, without compromising myocardial contractility or atrio-ventricular conduction characteristics, they might be beneficial in the treatment of ischemic heart disease (Baiker *et al*., 1991).

In cardiac tissue, it has been demonstrated that sinus node inhibitors reduce the hyperpolarization-activated current $I_f$ (Snyders & van Bogaert, 1987; Goethals *et al*., 1993; van Bogaert *et al*., 1990). The current activates upon hyperpolarization of the membrane, is carried by sodium and potassium and does not show inactivation (DiFrancesco, 1985). In the SA node it provides inward current during the diastolic depolarization phase of spontaneous activity (DiFrancesco, 1991). It was demonstrated in isolated rabbit sino-atrial node cells that the sinus node inhibitor UL–FS 49 blocked $I_f$ in a use-dependent manner, which coincided with the slowing of the diastolic depolarization rate. Therefore the bradycardic effect of the drug might be explained by block of $I_f$ (Goethals *et al*., 1993).

A similar hyperpolarization-activated current, $I_h$, has also been described in both central and peripheral nervous tissue (for review see Pape, 1996). Like the sino-atrial node, it has been proposed that $I_h$ could support the rhythmicity of neurons (McCormick & Pape, 1990; MacCaferri & McBain, 1996). However, in an extensive clinical study with UL–FS 49 only one type of side effect, specifically related to the visual system, was observed (Frishman *et al*., 1995). This might indicate that (1) the pharmacological profile of sinus-node inhibitors is different for $I_f$ compared to $I_h$. Indeed, it has been demonstrated that DH–AH 268 and UL–FS 49 blocked $I_h$ in dorsolateral geniculate neurons (LGNd) (Pape, 1994) with an effective dose which is about 1000 fold higher compared to cardiac tissue (van Bogaert *et al*., 1990). However, the amount of block, in cardiac tissue, was strongly dependent on the pulse protocols. Therefore we studied the drug channel interactions with a similar approach as performed in cardiac tissue. (2) The lack of side-effects might also indicate that $I_h$ plays a minor role in the nervous system, despite its widespread expression. Therefore we investigated the role of $I_h$ in DRG neuron's electrical activity by blocking it with sinus-node inhibitors as well as with $Cs^+$.

[2]Current address: Laboratory of Molecular Biophysics, Physiology and Pharmacology, Department of Biochemistry, University of Antwerp (UIA), B-2610 Wilrijk, Belgium.
[3] Author for correspondence at: Laboratory of Molecular Biophysics, Physiology and Pharmacology, Department of Biochemistry, University of Antwerp (UIA), B-2610 Wilrijk, Belgium.

We could demonstrate that $I_h$ was blocked by the sinus node inhibitors, UL–FS 49 and DK–AH 269 at doses comparable as described for cardiac tissue. However, the kinetics of block and unblock are more complicated compared to cardiac tissue and might be explained by the existence of two subtypes of channels. Previously we could demonstrate that $I_h$ was activated at the resting membrane potential (Raes et al., 1997). By measuring the membrane potential and stimulating the cell we could demonstrate that $I_h$ is functionally preventing hyperpolarizations of the membrane after a stimulus train. Part of the results appeared in abstract from Raes & van Bogaert (1996).

## Methods

DRG neurons were isolated from 12–14-day-old mouse embryos (E12–E14). The cells were subsequently kept in culture for 4–6 weeks (see Ransom *et al.*, 1977). For our recordings cells with a spherical shape, a diameter from 30–50 $\mu$m and a distinct nucleus were chosen.

All recordings were performed at room temperature. The recording chamber consisted of a culture dish in which a teflon ring was placed to reduce the volume. This was mounted on an inverted microscope (Zeiss IM 35). The cells were continuously superfused with extracellular solution. The recording chamber was grounded with a Ag-AgCl pellet. The Axoclamp 2A current-voltage amplifier (Axon Instruments) was connected to a Labmaster TL-1 DMA interface (Scientific Solutions). Measurements were performed in the whole-cell mode of the patch-clamp technique. Electrodes were pulled from 1.7 mm diameter glass capillaries (Jencons, H15/10) and heat polished with a Brown Flaming P-87 horizontal pipette puller. The electrodes with resistances of 2–4 MΩ were filled by dipping in an internal solution and by backfilling. The internal solution was filtered through a 0.22 $\mu$m filter. The electrode was positioned by a micromanipulator. Seal formation (at least 5 GΩ) was performed by suction and was monitored on an oscilloscope. The membrane patch was ruptured by a suction pulse. Single electrode voltage-clamp was performed in the discontinuous mode with a sample rate below 3–4 kHz, which was optimal, as monitored on a second oscilloscope. In the case that the $K^+$ concentration was increased to 20 mM the two electrode voltage clamp mode was applied. With this solution the current amplitude was increased by 2–3 fold, which could not be clamped accurately with the single electrode voltage clamp mode. The capacitance was measured with small voltage steps of 5 mV. All data were corrected for the liquid junction potential which amounted to 7.8 mV, measured as described by Neher (1992).

Extracellular solution contained (in mM): 140 NaCl; 5 KCl; 1.8 $CaCl_2$; 1 $MgCl_2$; 5 HEPES; 10 Glucose; 0.5 $\mu$M TTX (Tetrodotoxin) with the pH adjusted to 7.4 with NaOH. The osmolarity was adjusted to 315–320 with sucrose. In some experiments 15 mM KCl was added to the normal solution to magnify the current and to obtain a measurable current after steady-state block. In that case 5 mM $BaCl_2$, a blocker of $I_{K,1}$, was added as, occasionally in this solution, an inward rectifier, different from $I_h$, was observed. In those cases no sucrose was added and NaCl was lowered by 10 mM to obtain the same osmolarity. The internal solution contained (in mM): 20 KCl; 110 K-aspartate; 1 $CaCl_2$; 2 $MgCl_2$; 2 EGTA; 5 $Na_2ATP$; 10 HEPES and 0.1 cyclic AMP with the pH adjusted to 7.4 with HCl. The osmolarity was adjusted to 315–320 with sucrose. The drugs (Figure 1) UL–FS 49 or 1,3,4,5-tetrahydro-7,8-dimethoxy-3-[3-[[2-(3,4-dimethoxyphenyl)ethyl] methyl-imino]-propyl]-2*H*-3benzazepin-2-*on*-hydrochoride and DK–AH 269 or (R)-(−)-1,3,4,5-tetrahydro-7,8-dimethoxy-3-[[1-[2-(3,4-dimethoxyphenyl)-ethyl)-3-piperidinyl]-methyl]-2*H*-3benzazepin-2-*on*-hydrochoride were kindly provided by the company Dr Karl Thomae GmbH, Biberach, Germany, and were added to the solution from a stock solution of 1 mM in $H_2O$ or were directly dissolved in the external solution in the case of high concentrations. CsCl (2 mM) was used to block $I_h$. Dihydroouabaine (DHO) was used in an attempt to block the $Na^+/K^+$ pump.

Data were digitized on line and stored on a hard disk of an IBM-compatible computer. Voltage-clamp step protocols were given by pClamp 5.6 and 6.03 software (Axon Instruments). Data were filtered at 1 kHz with a Butterworth filter (Kemo, VBF803) before digitizing. pClamp and other conventional software were used to analyse the data. Data are presented as means ± s.e.mean ($n$), where s.e.mean is the standard error of the mean and $n$ the number cells. Currents were normalized to cell capacitance. Significance of differences between the means of two groups was tested with a Student's $t$-test. In the case of membrane potential and resistance measurements the data were pair-wise evaluated. The level of significance $P$ was chosen as 0.05.

## Results

### *The block of $I_h$ by UL–FS 49 and DK–AH 269 is use-dependent*

The drugs UL–FS 49 and DK–AH 269, which is the left and more potent stereo isomer of the racemic mixture DK–AH 3, block the pacemaker current, $I_f$, in heart tissue in a use-dependent manner, at low doses ($K_d$ of 0.06 $\mu$M in Purkinje fibers and 0.5 $\mu$M in SA node cells for UL–FS 49 and $K_d$ of 8 nM in Purkinje fibers for DK–AH 3) (Goethals *et al.*, 1993; van Bogaert *et al.*, 1990; van Bogaert & Raes, 1993). Since $I_h$ shows high similarity to cardiac $I_f$, we investigated the effect of UL–FS 49 and DK–AH 269 on this current in a similar way. Therefore a voltage-clamp protocol was applied as is shown in Figure 2A. The membrane voltage was stepped from −38 mV, where $I_h$ is deactivated, to −108 mV, where almost complete activation occurs. Representative current recordings are shown in Figure

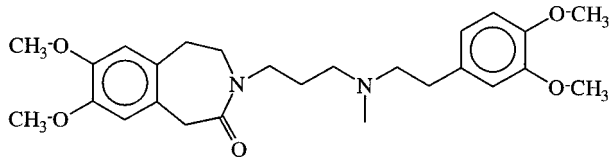


UL-FS 49

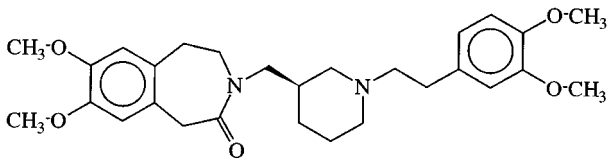


DK-AH 269

**Figure 1** Molecular structure of the sinus node inhibitors UL-FS 49 and DK-AH 269.

2B. After an instantaneous current jump, $I_h$ slowly activated and showed no inactivation. Upon stepping back to −38 mV, only a very small tail current was observed as this is close to the reversal potential. When a voltage-clamp pulse train was applied at 0.5 Hz in control conditions, no changes in current amplitude were observed (data not shown). Afterwards the cell was clamped at −38 mV and the drug was superfused for at least 3 min. To investigate the use-dependent block, the same pulse train was applied. During the first hyperpolarizing step in the presence of 5 μM DK–AH 269, the instantaneous current jump was identical to the one in control conditions. The time-dependent component, $I_h$, was only blocked by a small amount (Figure 2B, N = 1) which was slightly dependent on concentration, ranging from not detectable, with 0.05 μM, to 4.8 ± 1.3% ($n = 6$) with 10 μM. Upon application of consecutive hyperpolarizing steps, the current decreased gradually and reached a steady-state block. The small amount of time-dependent current that remained at steady-state, could be blocked by extracellular application of 2 mM $Cs^+$ (which is known to block the inward $I_h$ current instantaneously). This indicated that $I_h$ was almost completely blocked by DK–AH 269 (Figure 2B). Figure 2C illustrates the decrease of the normalized current as a function of the pulse number in the same cell. This reduction was well fitted by a single exponential function, as is represented with the continuous curve, and a pulse constant (i.e. the number of pulses needed to obtain an e-fold reduction of the normalized current) was obtained. With UL–FS 49 similar results were obtained, although with higher concentrations. The steady-state use-dependent block, obtained at the end of the pulse train, increased with higher concentrations of DK–AH 269 and UL–FS 49. This is shown in Figure 3 where a logarithmic concentration response curve is represented. The apparent $K_d$ obtained, was 0.1 μM and 0.79 μM with a slope factor of 0.86 and 0.69 with DK–AH 269 and UL–FS 49 respectively. The rate of block is obtained from the single exponential approximation as in Figure 2C and was dependent on concentration. In Figure 4 the inverse of the pulse constant (i.e. the blocking rate, defined as $\lambda$) is shown as a function of drug concentration. It increases linearly with increasing drug concentration with a slope of $4.1 \times 10^3$ $N^{-1}$ $M^{-1}$ and $1.0 \times 10^4$ $N^{-1}$ $M^{-1}$ and an intercept of $1.6 \times 10^{-3}$ $N^{-1}$ and $2.1 \times 10^{-3}$ $N^{-1}$ with DK–AH 269 and UL–FS 49 respectively.

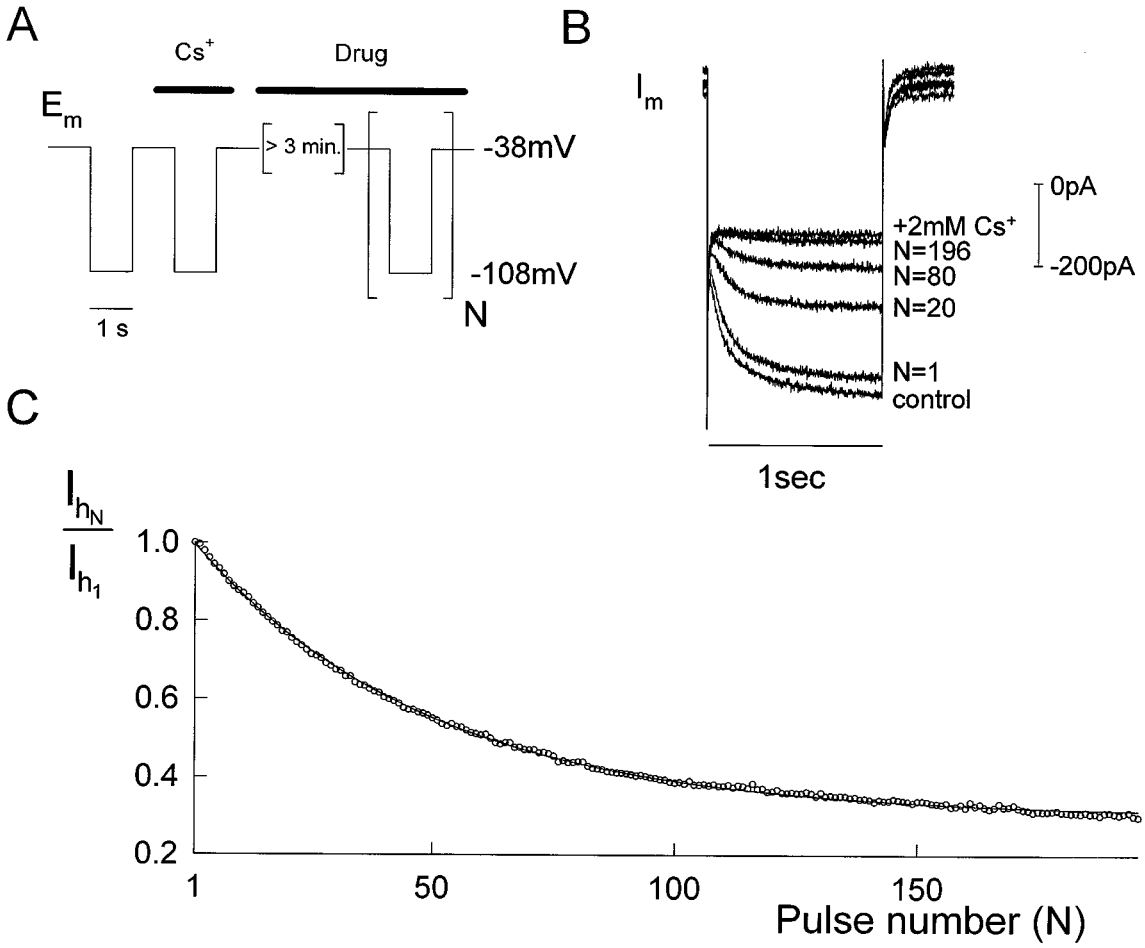


**Figure 2** Use-dependent block of $I_h$ with 5 μM DK-AH 269. (A) Protocol used to obtain use-dependent block. The membrane was clamped at −38 mV and a test pulse of 1 s to −108 mV, to activate $I_h$, was applied in control conditions and in the presence of 2 mM extracellular $Cs^+$, to block $I_h$. Afterwards the drug was applied for at least 3 min while the membrane was clamped at −38 mV, before a pulse train of 0.5 Hz to −108 mV was applied, with N indicating the number of pulses. (B) Currents recorded with a pulse protocol as shown in part A. The current traces recorded at pulse number N, in the presence of 5 μM DK-AH 269, are superimposed on those recorded in control conditions and in the presence of 2 mM of $Cs^+$. Only a small tonic block was observed (N = 1). (C) Decrease of the current is represented as function of the pulse number. The amplitude of $I_h$ was normalized to the amplitude recorded at the first pulse. The decrease fitted well with a single exponential function with a pulse constant of 47.9 pulses in this case.

*Effect on activation curve and instantaneous I-V relation*

The experiments to study the effect of the drugs on the activation curve and on the fully-activated current-voltage relation, were performed in a modified solution with extracellular $K^+$ increased to 20 mM in order to magnify the current and to obtain a measurable current after steady-state block. The activation curve was obtained by a voltage-clamp protocol, as shown in the inset of Figure 5A. Hyperpolarizing prepulses, between −53 mV (holding potential) and −123 mV with varying duration (inset, Figure 5A), were applied to evoke $I_h$. The activation curve of $I_h$ was calculated from the peak amplitude of the tail currents recorded at −128 mV (similar as described in Kamondi & Rainer (1991) (inset, Figure 5A). Tail current amplitudes ($I_{h,tail}$) and tail currents normalized to the maximal tail current ($I_{t,max}$), were plotted against the prepulse voltage (Figure 2A,B). The activation curve was approximated by a Boltzmann curve with a midpoint potential of −79.2±3.7 mV ($n=3$) and a slope of 7.0±0.5 mV ($n=3$). After >3 min of perfusion of 1 μM UL-FS 49, approximately 50% block was induced with a pulse train of 150 pulses, as shown in Figure 2A. The activation curve was not shifted (Figure 5B) and the midpoint potential and slope amounted respectively to −80.3±4.2 mV and 7.8±0.3 mV ($n=3$) which was not significantly different.

To study the effect on the fully-activated current-voltage relation of the h-channel, a voltage-clamp protocol was applied, as is shown in the inset of Figure 6. The membrane was hyperpolarized for 750 ms to at least −128 mV, where $I_h$

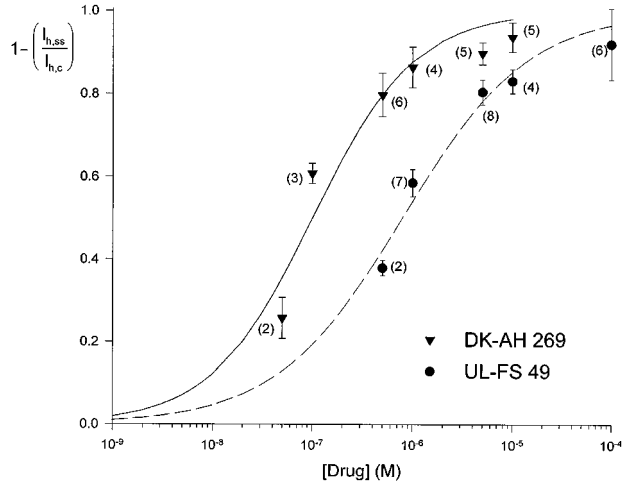


**Figure 3** Concentration-response curve for use dependent block. Steady state block was induced by the same voltage protocol as shown in Figure 1A. The fraction of block at steady-state was calculated as one minus the ratio of the amplitude of blocked current at steady-state and the amplitude in control solution. In both cases the $Cs^+$-sensitive current was used. The block is represented as function of the logarithm of the drug concentration. The results were fitted with the expression $y=1-[1+(K_d/x)^n]^{-1}$ which resulted in a $K_d$ of approximately 0.1 and 0.79 μM and a slope of 0.86 and 0.69 with DK-AH 269 and UL-FS 49 respectively. Values represent means±s.e.mean, with the number of experiments indicated between brackets.

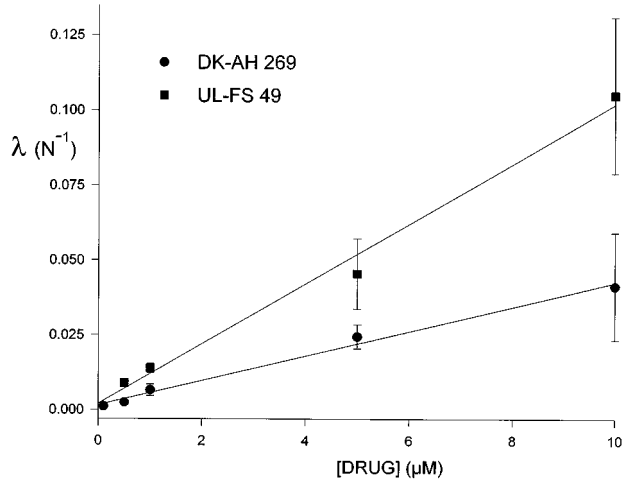


**Figure 4** Rate of use-dependent block plotted as function of drug concentration. The rate ($\lambda$) is obtained as the inverse of the pulse constant which is determined by an exponential fit of the time dependent current decrease as shown in Figure 1C. Results are fitted with a straight line with a slope of $4.1\times10^3$ and $10^4$ $N^{-1}$ $M^{-1}$ and an intercept of $1.6\times10^{-3}$ and $2.1\times10^{-3}$ $N^{-1}$ with DK-AH 269 and UL-FS 49 respectively.

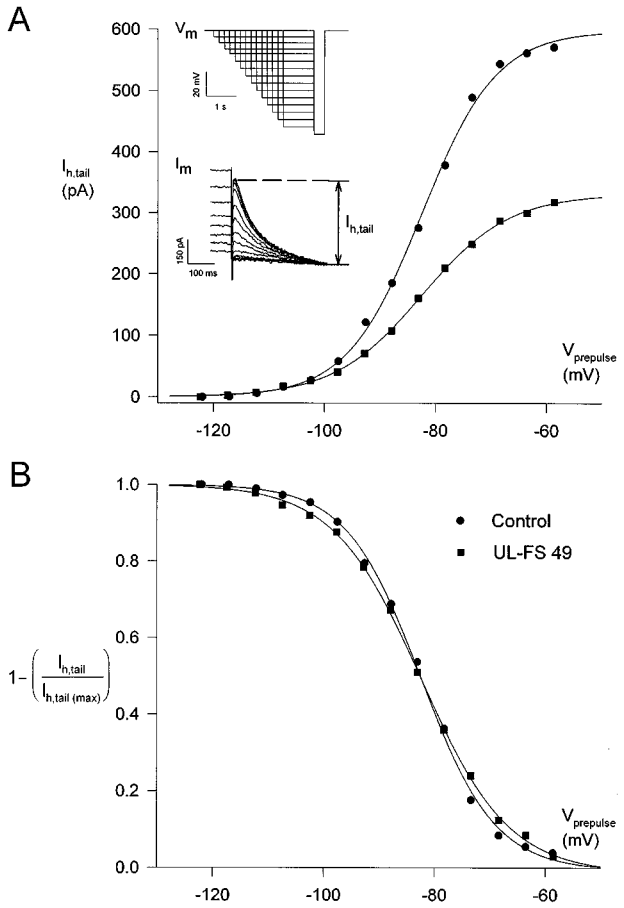


**Figure 5** Effect of UL-FS 49 on the activation curve of $I_h$. (A) The activation curve was calculated with current recordings obtained with a voltage-clamp protocol as shown in the inset. Hyperpolarizing prepulses, lasting from 3.4 s to 1.2 s, between −53 mV (holding potential) and −123 mV, were applied to activate $I_h$. Afterwards a hyperpolarizing step to −128 mV, to obtain complete activation, was applied. The activation curves were obtained by plotting tail current amplitudes, as shown in the inset, as a function of the prepulse voltage. Two examples of activation curves in control conditions (●) and after steady-state block in the presence of 1 μM UL-FS 49 (■) are shown. The data were fitted with a Boltzmann curve with a midpoint potential of −82.6 and −82.7 and a slope of 6.6 and 7.7 mV in control conditions and after steady-state block with UL-FS 49. (B) Same data as in panel A but normalized between tail current amplitudes observed at −128 and −58 mV.

is fully-activated, and is stepped back to different potentials. The leakage conductance was obtained by application of 2 mM $Cs^+$ in the bath solution and was subtracted off-line. The instantaneous tail current amplitude of the leak corrected current reflects net $I_h$ through fully activated channels and is plotted against the voltage at which the tail is measured (Figure 6). The relation was approximated by a linear regression and the slope conductance, after scaling to cell capacitance, amounted to $0.45 \pm 0.13$ nS/pF ($n=4$). Afterwards, $I_h$ is blocked by a voltage-clamp pulse train, as represented in Figure 2A by 1 $\mu$M UL–FS 49. After reaching steady-state block, the protocol is repeated. It is clearly shown that the conductance is significantly reduced to $0.14 \pm 0.08$ nS ($n=4$) without shifting the reversal potential of $-32.1 \pm 5.7$ mV in control conditions and of $-34.1 \pm 6.1$ mV ($n=4$) after steady state block.

### *Unblock of $I_h$ occurs with sustained hyperpolarizations*

After induction of use-dependent block with a voltage-clamp protocol as shown in Figure 2A, some relief of block could be observed, in the presence of UL–FS 49, by hyperpolarizing the membrane for a prolonged period of time. The unblock was obtained by clamping the membrane at hyperpolarizing voltages, ranging from $-108$ to $-138$ mV, for 20 s and was subsequently quantified by a test pulse of 1 s at $-108$ mV (Figure 7). During the hyperpolarizing step of 20 s, the current amplitude increased slowly. When this protocol, 20 s step and test pulse, was repeated more unblock which was observed by the increase of the amplitude of the test pulse to $-108$ mV. In Figure 7B the current amplitude at $-108$ mV was plotted as a function of the time spent at the hyperpolarizing voltage (obtained in segments of 20-s steps). The amount of relief from block, obtained at steady-state, was difficult to determine as a lot of cells deteriorate by long hyperpolarizations. In all cases it was less than 30% ($n=2$), at $-138$ mV, of the fraction of use-dependent blocked current. The rate of unblock was dependent on the voltage and its time course could be approximated by a single exponential function (Figure 7). The time constant amounted to $61 \pm 11$ s ($n=2$); $99 \pm 16$ s ($n=5$); $155 \pm 5$ s ($n=5$) at $-138$, $-128$ and $-108$ mV respectively. After wash-out (>10 min) a small increase (<10%) of $I_h$ was observed (data not shown).

### *Block of the open channel*

In order to demonstrate the association of the drug to the open channel, a custom-made fast perfusion system was used. The speed of the solution change was checked by the application of $Cs^+$ at hyperpolarized potentials (Figure 8). The block by $Cs^+$ could be described with a single exponential function with a time constant of $207 \pm 23$ ms ($n=20$). The UL–FS 49 concentration was increased in order to obtain steady-state block within an acceptable time scale. The protocol used is depicted in Figure 8. $I_h$ is activated by stepping the membrane voltage to $-108$ mV and, after reaching steady-state, a brief pulse of $Cs^+$ was applied to obtain the net $I_h$ amplitude. Upon application of 2 mM UL–FS 49, a decrease in inward current was observed, which was best described with a double exponential function. This demonstrated the association of UL–FS 49 with the open channel. In control conditions the current amplitude did not change during the long hyperpolar-

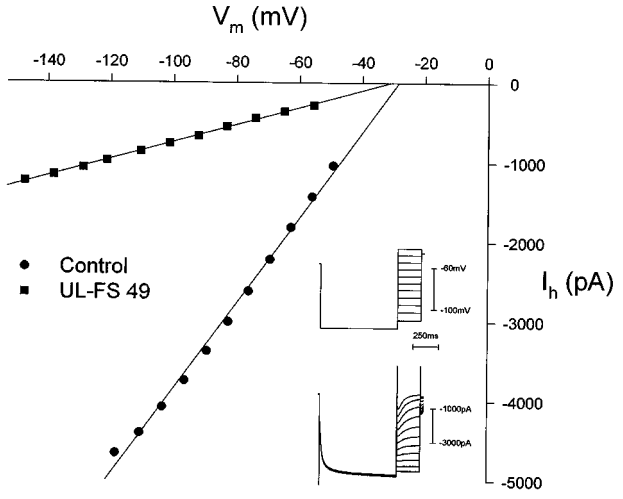


**Figure 6** Effect of UL-FS 49 on the fully-activated current-voltage relation. The protocol and current recordings used to calculate the fully-activated current voltage relation are shown in the inset. After a prepulse to at least $-128$ mV, tail currents were recorded at different voltages. After blocking $I_h$ with a 1 $\mu$M UL-FS 49 as shown in Figure 2A the protocol was repeated. The fully-activated current-voltage relation in control conditions (●) and after being blocked (■) was obtained by plotting the leakage-corrected instantaneous tail current amplitudes as a function of the voltage. The data were fitted with a straight line with a slope and a reversal potential of respectively 54 pA $mV^{-1}$ and $-28.8$ mV in control conditions and of 10.7 pA $mV^{-1}$ and $-31.8$ mV after reaching steady-state block.

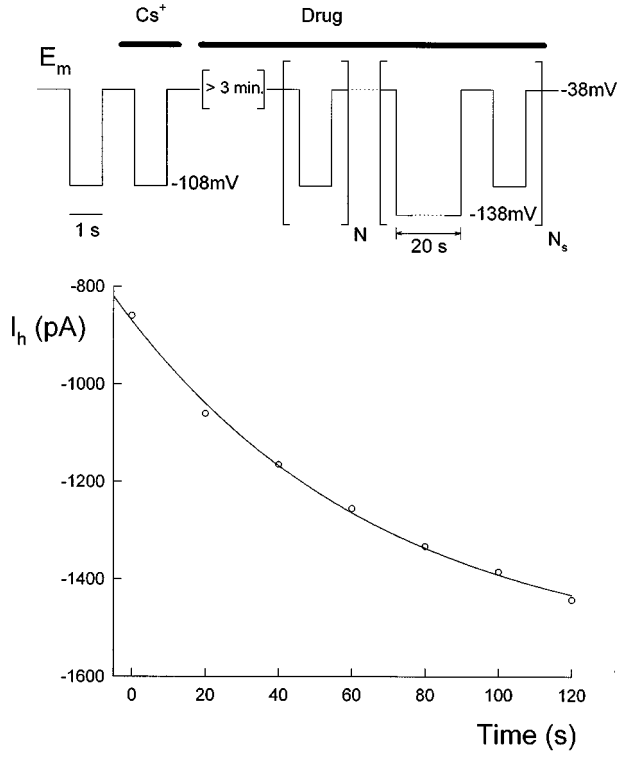


**Figure 7** Unblock at hyperpolarized potentials in the presence of UL-FS 49. The protocol to obtain block and unblock of $I_h$ in the presence of 1 $\mu$M UL-FS 49 is shown on top. The steady-state amplitude of $I_h$ was measured with a pulse of 1 s to $-108$ mV after reaching steady-state block with a train of N pulses. Afterwards, the membrane was clamped at $-138$ mV for 20 s and a test pulse to $-108$ mV was applied. Both pulses were applied repetitively ($N_s$) and the amplitudes obtained with the test pulse (○) were plotted as a function of the amount of time the membrane was clamped at $-138$ mV (obtained by summed 20-s pulses). The data were approximated by a single exponential with a time constant of 70.9 s at $-108$ mV (test pulse). Note the current size, compared with Figure 6 (same cell).

izations. Afterwards, the solution was changed to a standard solution and a significant recovery of inward current was observed. A short $Cs^+$ pulse was applied again to check for an increase of leakage current. The average steady-state block amounted to $87.3\pm1.1\%$, $80.4\pm3.6\%$, $77.7\pm2.3\%$ and $67.1\pm3.5\%$ in 2, 1, 0.5 and 0.1 mM UL–FS 49 respectively. The estimated $K_d$ for open channel block at $-108$ mV was 13 $\mu$M. The fast and the slow time constant associated with this open channel block, were dependent on the concentration of UL–FS 49 and amounted for $\tau_f$ and $\tau_s$ to $9.2\pm1.3$ s and $96.8\pm11.4$ s, $2.7\pm0.5$ s and $22.3\pm2.9$ s, $2.1\pm0.2$ s and $14.4\pm2.3$ s, $1.4\pm0.7$ s and $10.6\pm0.8$ s in 0.1, 0.5, 1 and 2 mM UL–FS 49 respectively. When the apparent rate constants were plotted as a function of drug concentration, the data were not satisfactorily described by a straight line, which indicates that this process cannot be described by a first order blocking scheme. When the drug was removed, a current increase was observed. This wash-out amounted to $43.8\pm3.4\%$ ($n=4$) of the blocked $I_h$-fraction with 2 mM of UL–FS 49. In another cell the protocol was slightly changed. This is shown in Figure 8B. Before the wash-out of UL–FS 49, a short depolarization to $-33$ mV (where $I_h$ channels are closed) was applied. In this case, a small additional block was observed after the depolarization and the recovery from block by wash-out was significantly smaller ($10.4\pm1.6\%$; $n=3$).

## *Physiological role of $I_h$*

*Membrane properties* Under current clamp conditions the average resting membrane potential amounted to $-63.3\pm1.0$ mV ($n=19$) in control conditions. Upon application of 2 or 10 mM extracellular $Cs^+$ the cell hyperpolarized significantly to $-69\pm1.8$ mV ($P=0.007$, $n=13$) and to $-68.1\pm1.8$ mV ($P=0.013$, $n=13$) respectively. When $I_h$ was blocked with a voltage clamp pulse train as shown in Figure 2 in the presence of 5 and 10 $\mu$M UL–FS 49, the membrane potential also hyperpolarized significantly to $-71.2\pm2.0$ mV ($P=0.02$, $n=6$) and to $-68.7\pm1.6$ mV ($P=0.014$, $n=7$) respectively. No significant differences were observed between application of different concentrations of $Cs^+$ or UL–FS 49 ($P>0.05$). Simultaneously with the hyperpolarization of the membrane potential an increase in the membrane resistance ($R_m$), at the resting membrane potential, was observed. In control conditions $R_m$ amounted to $169\pm19$ MΩ ($n=19$) which increased (see also Figure 9, compare left and right of panel B) by $62\pm14\%$ ($P=0.004$, $n=11$), $69\pm15\%$ ($P<0.001$, $n=13$), $79\pm35\%$ ($P=0.023$, $n=7$), $90\pm40\%$ ($P=0.006$, $n=7$) with 2 and 10 mM $Cs^+$ and with 5 and 10 $\mu$M UL–FS 49 respectively. Again, no significant differences were observed between application of different concentrations of $Cs^+$ or UL–FS 49 ($P>0.098$).

*Action potential* When the cells were stimulated, above the threshold level, with a constant current pulse of 1.5 nA and a duration of 0.5 ms, typical action potentials (Figure 9) of 4 ms duration (90% repolarization) with an amplitude of 110 mV were elicited. After the action potential spike a significant after-hyperpolarization and subsequent slow return to the

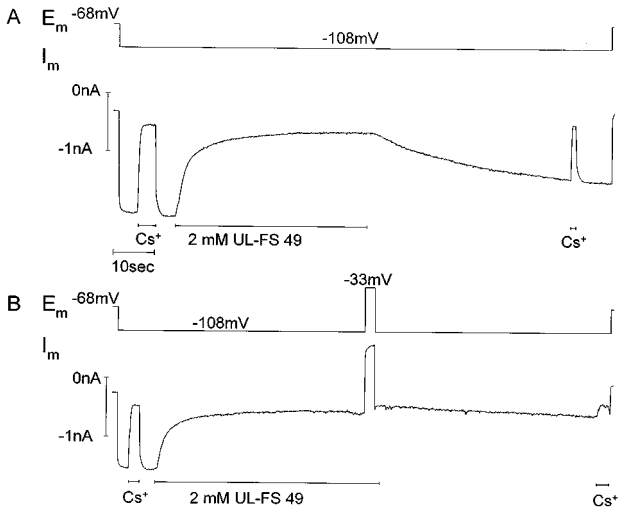


**Figure 8** Block of the open channel by UL-FS 49. (A) The voltage clamp protocol is shown on top. The membrane was clamped from $-68$ mV to $-108$ mV to activate $I_h$. The current recording is shown underneath. After the activation of $I_h$ a pulse of $Cs^+$ was applied and a complete block of the current was observed, which was reversed by removal of $Cs^+$. After application of 2 mM of UL-FS 49 a current block of 95% was observed. This decrease of the current was well approximated by a double exponential function. After removal of the drug a substantial recovery was observed. A second pulse of $Cs^+$ was applied to check for rundown. (B) Same protocol as described in panel A but after application of the drug a 1-s depolarization to $-33$ mV was applied. The recovery was much smaller as compared to panel A. Note that the depolarization prevents recovery from block while a current block by $Cs^+$ did not (second $Cs^+$ pulse in panel A).

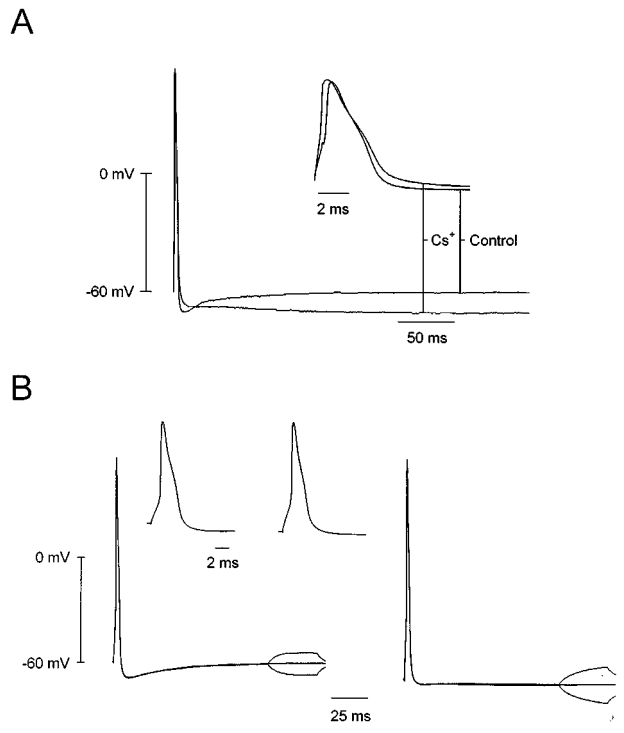


**Figure 9** Effect of $Cs^+$ and UL-FS 49 on the action potential. (A) Typical action potentials were recorded in physiological conditions and consisted of a brief transient depolarization to $+52.2$ mV. Afterwards, a transient hyperpolarization, followed by a slow return to the resting potential, is observed. In the presence of 10 mM $Cs^+$ the hyper- and depolarization, observed after the action potentials, are absent. The inset shows the same data on an enlarged time scale. Note the faster rise time with the onset of the current stimulus, as a consequence of the increased resistance, in the presence of $Cs^+$, while the shape of the action potential is unaffected. (B) Three superimposed action potentials recorded in control conditions (left) and after block of $I_h$ (right) in the presence of 10 $\mu$M UL-FS 49 following a voltage-clamp pulse protocol as shown in Figure 2. The inset shows the same data on an enlarged time scale. A small positive and negative current pulse at the end of the recording demonstrates the increase in membrane resistance and time constant.

resting potential was observed in most cells (Figure 9A,B). Upon extracellular application of 2 mM $Cs^+$ the resting membrane potential hyperpolarized, the after-hyperpolarization and subsequent slow return to the resting potential disappeared while the action potential spike did not change (Figure 9A). Similar results were obtained after blockade of $I_h$ with a voltage clamp pulse train in the presence of 5 or 10 $\mu$M UL–FS 49 (Figure 9B).

*Repetitive stimulation* To mimic the stimulation of a cell *in vivo* a stimulus train of more than 100 pulses, at a frequency of 3 Hz, was applied to evoke action potentials. In control conditions, the after-hyperpolarization and subsequent slow return to the resting potential, as well as the action potential, were identical during the stimulus train. Also the membrane potential, recorded after the stimulus train, was stable, and not different from the one, recorded before the stimulus train (data not shown). On the other hand, when the same protocol was applied in the presence of 2 mM $Cs^+$ in the extracellular solution, the membrane potential hyperpolarized slowly between the action potentials. This hyperpolarization increased with every successive action potential in the train and reached a steady state value. After the stimulus train the hyperpolarization reached a maximum of $-76.6\pm3.1$ mV ($n=10$) and a slow return to the resting membrane potential was observed. This maximum which is further referred as $V_{m,max}$ was significantly hyperpolarized compared to the resting membrane potential measured before the stimulus train ($P<0.001$). $V_{m,max}$ was more pronounced ($-96.3\pm3.7$ mV, $P<0.001$, $n=12$) when 10 mM of $Cs^+$ was applied (Figure 10). Also when $I_h$ was blocked with a voltage clamp pulse train, in the presence of 5 or 10 $\mu$M UL–FS 49, the membrane potential hyperpolarized between the action potentials and $V_{m,max}$ amounted to, respectively, $-79.4\pm3.0$ mV ($P=0.003$, $n=6$) and $-77.7\pm3.2$ mV ($P=0.003$, $n=6$) which was significantly hyperpolarized compared to the resting membrane potential measured before the stimulus train. Thus, when $I_h$ is blocked by $Cs^+$ or by UL–FS 49, the membrane potential hyperpolarized between the action potentials and a $V_{m,max}$ is observed after a stimulus train while both phenomena were not present in control conditions. As $V_{m,max}$ (maximum of $-120.8$ mV with 10 mM $Cs^+$) was more negative compared to the Nernst potential of $K^+$, which amounted to $-83$ mV, we speculate that this could result from the activation of the electrogenic $Na^+/K^+$ pump. To investigate this further 10 $\mu$M DHO (Dihydrooubaine, a blocker of the $Na^+/K^+$ pump) was applied in the presence of 2 or 10 mM $Cs^+$ or 10 $\mu$M UL–FS 49 ($I_h$ blocked with a voltage clamp pulse train). In these cases the values of $V_{m,max}$ were not significantly different from the ones observed without DHO and amounted respectively to $-87.2\pm6.7$ mV ($P=0.7$, $n=3$), $-110.6\pm3.8$ mV ($P=0.1$, $n=5$) and $-83.2\pm5.6$ mV ($P=0.12$, $n=4$). However, the potency of DHO in DRG neurons is low. Therefore we inhibited the $Na^+/K^+$ pump by excluding $K^+$ from the extracellular solution. In these conditions, when $I_h$ was blocked with a voltage clamp pulse train in the presence of 10 $\mu$M UL–FS 49, the membrane potential did not hyperpolarize between the action potentials and $V_{m,max}$ was not observed. The membrane potential after the stimulus train amounted to $-73.8\pm1.3$ mV and was not significantly different from the value before the stimulus train ($P=0.17$, $n=3$).

Finally to investigate whether sinus-node inhibitors could block $I_h$ *in vivo*, thus without a 'special' voltage clamp pulse train, we applied 1 $\mu$M UL–FS 49 in the extracellular solution while the cells were continuously stimulated at 3 Hz. The membrane resting potential was significantly hyperpolarized to $-70.8\pm3.3$ mV after 1800 pulses, compared to control conditions ($-63.5\pm2.8$ mV, $P=0.048$). This hyperpolarization was associated with a significant ($P=0.023$) increase in membrane resistance, at the resting membrane potential, to $132\pm5\%$ ($n=4$) while $I_h$, measured with a test pulse from $-38$ to $-88$ mV, was significantly decreased to $34\pm8\%$ ($P=0.003$, $n=4$) compared to control conditions.

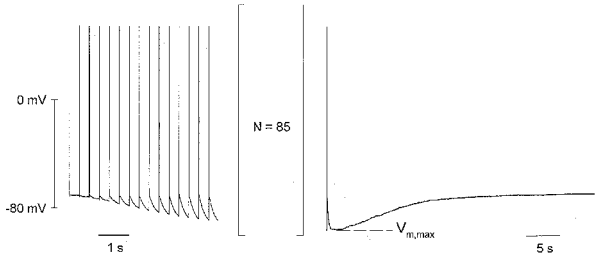


**Figure 10** Examples of action potentials recorded with a stimulus train of 103 pulses, in the presence of 10 mM $Cs^+$. The first 15 and last three action potentials are shown, with N indicating the number of action potentials not shown. Note the increasing hyperpolarization, observed after an action potential, during the pulse train. After the stimulus train the membrane hyperpolarized transiently to $-95.8$ mV ($V_{m,max}$) and slowly returned to the resting level.

## Discussion

These results demonstrate that UL–FS 49 and DK–AH 269 are powerful blockers of the hyperpolarization-activated current, $I_h$, in mouse DRG neurons. The characteristics of block are comparable with those observed on $I_f$, a similar current in cardiac tissue (van Bogaert *et al*., 1990; Goethals *et al*., 1993) and on h-channels in thalamo-cortical relay neurons (Pape, 1994). The block is use-dependent and is associated with a reduction of the slope of the fully-activated I/V relationship without shifting the activation curve along the voltage axis and thus probably acting only on the conductance while the gating characteristics are unaffected. In mouse DRG neurons the $K_d$ with UL–FS 49 is comparable with the one obtained in cardiac SA node cells (Goethals *et al*., 1993) but is more than a magnitude higher compared to the $K_d$'s for DK–AH 3 and UL–FS 49 in cardiac Purkinje fibers (van Bogaert *et al*., 1990; van Bogaert & Raes, 1993). However, compared with the concentration range from 10–1000 $\mu$M required for block in relay neurons (Pape, 1994) the effective concentration in mouse DRG neurons is lower. This difference might originate (1) from the local application of these drugs, as these relay neurons were investigated *in vitro* in brain slices. (2) In contrast with our study, the least potent isomer DK–AH 268 (Van Bogaert & Raes, 1993) was used in relay neurons. (3) However, another explanation arising from the mechanism of block, cannot be excluded. As the block by these drugs is use-dependent, the effective dose depends on the pulse protocol utilized. In thalamic relay neurons (Pape, 1994) the stimulus interval amounted maximally to 0.125 Hz while we stimulated at 0.5 Hz. In cardiac Purkinje fibers the $K_d$ for block of $I_f$ with UL–FS 49 shifted from 0.45 to 0.08 $\mu$M by changing the stimulus interval from 0.04 to 0.8 Hz (van Bogaert *et al*., 1990).

Use-dependent block has been satisfactorily described by two mechanisms (for review see Hille, 1992). The modulated receptor theory explains use-dependent block by different binding and unbinding parameters for each of the states of the

channel (Hondeghem & Katzung, 1977; Hille, 1992). The guarded receptor theory gives an alternative explanation by considering binding sites which have fixed affinities but are not permanently accessible (Starmer, 1986). In cardiac Purkinje fibers, application of the guarded receptor theory provided an adequate explanation for the use-dependent block (van Bogaert *et al*., 1990). However, the use-dependent block observed in DRG neurons displayed different characteristics (compared to cardiac tissue) which did not allow the simplifications used in this tissue. For example: (1) The sum of the association rates constants is reflected by the slope of the $\lambda$-concentration curve while the sum of the dissociation rates is reflected by the intercept of this curve. Their ratio defines the apparent $K_d$. In cardiac Purkinje fibers a lower $K_d$ (DK – AH 3 compared to UL – FS 49) is accompanied by a 3 fold increase of the slope of the $\lambda$-concentration curve (van Bogaert & Raes, 1991) while in DRG neurons the opposite is observed; a more than 2 fold decrease with a reduced $K_d$ (DK – AH 269 compared to UL – FS 49). To explain this difference according to the guarded receptor theory (Starmer, 1986) the sum of unbinding rates, reflected by the intercept, should decrease which is not observed. (2) A major difference, observed between the effects of UL – FS 49 described in cardiac preparations (van Bogaert *et al*., 1990; Goethals *et al*., 1993) and in neurons (Pape, 1994 and our preparation) is the block of the open channel at high concentrations. In the DRG neuron the $K_d$ for the open channel block was estimated at 13 $\mu$M with a slow time constant of about 100 s, while in cardiac Purkinje fibers, in the presence of 20 $\mu$M, no significant decline of the current was observed after 4 min at $-120$ mV. Although the combination of a lower drug concentration with stronger hyperpolarizations (higher dissociation rates) may have minimized the open channel block in Purkinje fibers, an open channel block with a comparable $K_d$ compared to DRG neurons should be observable. As a consequence open channel block is much lower or not present in Purkinje fibers and allowed to describe the block with association of the drug to a single state, which in the case of DRG neurons is not possible. (3) Moreover, open channel block could not be described by a single exponential time course, suggesting that perhaps two kinetic processes are involved. However, we cannot exclude the possibility that one time constant originates from the perfusion system and that the increased value (compared to $Cs^+$ application) results from equilibration of the drug across the plasmalemma as the drug acts on the channel from the intracellular side (van Bogaert & Goethals, 1992). Nevertheless, the $\lambda$-concentration curves were not satisfactorily described by a straight line, indicating that this open channel block does not follow a first order blocking scheme. In thalamo-cortical projecting neurons it has been suggested that $I_h$ consists of two populations of channels (Solomon & Nerbonne, 1993). This was confirmed in cardiac tissue by a mutant Zebrafish which lacks one kinetic component (Baker *et al*., 1997). The double exponential observed with the open channel block might be explained by different sensitivities of these subtypes for bradycardic drugs.

In conclusion, the results obtained in DRG neurons are somewhat intermediate compared to cardiac SA node cells and Purkinje fibers. In the Purkinje fibre the low $K_d$ is associated with a slower unblock while for SA node cells the higher $K_d$ corresponds with an increased rate of unblock. The DRG neuron combines a slow unblock with a higher $K_d$ which might coincide with open channel block.

Several organic compounds have been shown to block $I_h$ or $I_f$ (Tokimasa *et al*., 1990; Perkins & Wong, 1995; DiFrancesco *et al*., 1991; BoSmith *et al*., 1993; Harris *et al*., 1994). Only specific bradycardic agents, such as UL – FS 49 (van Bogaert *et al*., 1990; Goethals *et al*., 1993) and S 16257 (Bois *et al*., 1996), potently ($10^{-9}$ to $10^{-6}$ M) inhibit the hyperpolarization activated current, both in cardiac tissue and in neurons. These compounds can thus be used to block $I_h$ or $I_f$ at low doses, which were ineffective for the blockade of other ion channels (Tytgat *et al*., 1992; Goethals *et al*., 1993; Raes *et al*., 1993), however other reports have shown the block of other ion channels at low doses as well (Doerr & Trautwein, 1990; Valenzuela *et al*., 1996).

At present several physiological functions have been attributed to $I_h$ such as setting the resting membrane potential, determining input resistance, providing 'pacemaker' current and preventing hyperpolarization (for review see Pape, 1996). Previously we have demonstrated that $I_h$ was activated at the resting membrane potential (Raes *et al*., 1997). By providing a steady inward current, $I_h$ keeps the resting membrane potential more depolarized compared to the Nernst potential of $K^+$, which has also been demonstrated for other neurons (Travagli & Gillis, 1994). Upon application of $Cs^+$ or UL – FS 49 (with or without a voltage clamp pulse protocol) this steady inward current is inhibited, as $I_h$ is blocked, and a hyperpolarization is thus observed. This hyperpolarization is dependent of intracellular cyclic AMP and thus the position of the activation curve (Raes *et al*., 1997). As $I_h$ is activated at the resting membrane potential it also contributes to the membrane resistance and membrane time constant, which is clearly observed in Figure 9B and which has also been demonstrated in intracardiac neurons (Cuevas *et al*., 1997).

It has also been proposed that $I_h$ contributes to oscillatory behavior of the cell. In cardiac SA node cells activation of $I_h$ during the diastolic interval depolarizes the membrane potential slowly to a threshold which results in an action potential (DiFrancesco, 1993). In neurons a similar behavior has been described in thalamo-cortical neurons (McCormick & Pape, 1990). These cells cycle between a burst of $Na^+/K^+$ spikes and slow hyperpolarization and a subsequent depolarization. In this scheme $I_h$ activates during the hyperpolarizing phase and provides inward current to depolarize the cell (Huguenard & McCormick, 1992). Furthermore, a model showed that $I_h$ was critical in the behavior at hyperpolarized potentials (McCormick & Huguenard, 1992). It also showed that tonic current input resulted in train of action potentials with little frequency adaptation and that shifting the voltage dependence of $I_h$ modulated this spiking behavior. Although DRG neurons do not display an oscillatory behavior, the steady inward current, provided by $I_h$ may result in keeping the neuron in a repetitive firing 'mode'.

The depolarizing 'sag' which is characteristic for the presence of $I_h$ has already been described years ago (Araki *et al*., 1962). Although the phenomenon clearly demonstrates an inhibitory effect of $I_h$ on hyperpolarizing inputs, such a role has, to our knowledge, never been demonstrated. When DRG neurons were stimulated repetitively, after block of $I_h$ with $Cs^+$ or UL – FS 49, a pronounced hyperpolarization (more negative than the Nernst potential of $K^+$) was observed after the stimulus train. Recently, such strong hyperpolarizations, sensitive to TTX were described in dLGN neurons (Pirchio *et al*., 1997). We could explain this hyperpolarization by the activation of the $Na^+/K^+$ pump, resulting from an increase of the intracellular $Na^+$ concentration during stimulation (Thomas, 1972), which is consistent with the sensitivity of this hyperpolarization for TTX observed in dLGN cells (Pirchio *et al*., 1997). This hyperpolarization in DRG neurons was not sensitive to the cardiac glycoside DHO at low concentrations, which can be explained by the low sensitivity ($K_d \sim 10^{-3}$,

Hermans, 1997) of the $Na^+/K^+$ pump current for DHO in these neurons. However, when extracellular $K^+$ was omitted from the bathing solution, thus preventing any pump activity, the hyperpolarization measured after a stimulus train with UL–FS 49, disappeared completely. As the extracellular binding site for $K^+$ of the $Na^+/K^+$ pump can be activated by extracellular $Cs^+$, it was not possible to inhibit the hyperpolarization observed in $Cs^+$ containing solutions by omitting $K^+$. Moreover, the increased hyperpolarization, observed in 10 mM $Cs^+$ compared to 2 mM $Cs^+$, can perhaps be explained by an increased pump activity (Isenberg, 1976; Sternlicht & Vasalle, 1995). In dLGN neurons this hyperpolarization is regularly observed in postnatal cells (P1-P9) while in adult cells it was mostly absent (Pirchio *et al*., 1997). Although $I_h$ is already detected as early as P2, no data are available for these neurons on the voltage dependence and amplitude of the current in relation to its input resistance and developmental age. The depolarizing sag was not always observed in young neurons and the amplitude was smaller and slower which might indicate a reduced $I_h$ or shifted voltage dependency. In DRG neurons $I_h$ is absent in early stages of development and is only expressed at later stages (Wang *et al*., 1997). In that perspective it is tempting to speculate that absence, a small amplitude or a voltage dependence shifted towards negative voltages is related to the variable hyperpolarizations observed in dLGN neurons. However, in dLGN neurons this hyperpolarization was reduced in amplitude and in duration by $Cs^+$ at more hyperpolarized potentials and it is blocked by $Cd^{2+}$ and $Co^{2+}$, (Pirchio *et al*., 1997). Although we have no data obtained with $Co^{2+}$ and $Cd^{2+}$, the hyperpolarization is clearly not reduced by $Cs^+$, on the contrary, which might point to a different mechanism in dLGN neurons. In conclusion, we propose that $I_h$ contributes to the resting membrane potential, but also counteracts hyperpolarizations, which can originate from an increased pump activity during stimulation. The subsequent inexcitability is thus prevented by h-channels as inwardly rectifying currents are absent in these DRG neurons (Scroggs *et al*., 1994).

SA node inhibitors were developed as a drug for treatment of ischemic heart disease (Kobinger & Lillie, 1987) and might be beneficial in the treatment of ischemic heart disease (Baiker *et al*., 1991). The main side effect of these products are visual disturbances such as light flashes and flickering (Frishman *et al*., 1995). These side effects can be explained by the action of the drug on the hyperpolarization activated current $I_h$, since this current is reported at various levels of the visual system (Wollmuth & Hille, 1992) and is blocked by these inhibitors at low concentrations. However, as $I_h$ is apparently expressed throughout the nervous system (for review see Pape, 1996), the lack of other side effects like dysesthesias and paresthesias, during treatment with UL–FS 49, is somewhat puzzling. This lack might be explained in several ways. (1) The position of the activation curve of $I_h$ on the voltage axis is dependent on the intracellular cyclic AMP concentration and on the phosphorylation state (Raes *et al*., 1997). As a consequence, the proportion of h-channels that are activated at the resting potential is modulated by the physiological state of the preparation. Thus, the presence of h-channels in a cell type, demonstrated in voltage clamp condition, does not necessarily imply that these channels also contribute to the resting membrane potential. (2) The time course of the spiking behavior in the nervous system is much faster than the spontaneous pacing in heart tissue, and perhaps $I_h$, which activates slowly, is not involved. However, in thalamic relay neurons h-channels contribute to intrinsic oscillations but in these cells it consists of slow oscillations (McCormick & Pape, 1990). (3) In the DRG neurons we have experimental evidence for a protective role of $I_h$ against hyperpolarizations and have previously shown that h-channels are activated at the resting potential, when the cytosolic content of the cell is not significantly altered (by using the nystatin patch method) (Raes *et al*., 1997). Although we have demonstrated that $I_h$ is blocked with UL–FS 49 by stimulating the cell (without a 'special' voltage clamp protocol), in a clinical study patients did not report adverse effects (Frishman *et al*., 1995). These findings might indicate that such a protective role only occurs in particular physiological conditions.

Further investigations are necessary to determine whether the varying presence of these side effects with different SA node inhibitors can be explained by the different sensitivity and differences in rate of block of $I_h$ current and/or the physiological role fulfilled by h-channels.

## References


ARAKI, T., ITO, M. & OSHIMA, T. (1962). Potential changes produced by application of current steps in motoneurones. *Nature,* **191,** 1104–1105.

BAIKER, W., CZAKO, E., KECK, M. & NEHMIZ, G. (1991). Efficacy and duration of action of three doses of zatebradine (UL-FS 49 Cl) in patients with chronic angina pectoris compared to placebo. In *Sinus node inhibitors. A new concept in angina pectoris*. Hjalmarson, Å. & Remme, W.J. (eds.). Springer Verlag: New York.

BAKER, K., WARREN, K.S., YELLEN, G. & FISHMAN, M.C. (1997). Defective 'pacemaker' current ($I_h$) in a zebrafish mutant with slow heart rate. *Proc. Natl. Acad. Sci. U.S.A.,* **94,** 4554–4559.

BOIS, P., BESCOND, J., RENAUDON, B. & LENFANT J. (1996). Mode of action of bradycardic agent, S 16257, on ionic currents of rabbit sino-atrial node cells. *Br. J. Pharmacol.,* **118,** 1051–1057.

BOSMITH, R.E., BRIGGS, I. & STURGESS, N.C. (1993). Inhibitory actions of ZENECA ZD7288 on whole-cell hyperpolarization-activated inward current ($I_f$) in guinea-pig dissociated sino-atrial node cells. *Br. J. Pharmacol.,* **110,** 343–349.

CUEVAS, J., HARPER, A.A., TREQUATTRINI, C. & ADAMS, D.J. (1997). Passive and active membrane properties of isolated rat intracardiac neurons: Regulation by H- and M-currents. *J. Neurophysiol.,* **78,** 1890–1902.

DIFRANCESCO, D. (1985). The cardiac hyperpolarizing-activated current, $I_f$. Origins and developments. *Prog. Biophys. Molec. Biol.,* **46,** 163–183.

DIFRANCESCO, D. (1991). The contribution of the 'pacemaker' current ($I_f$) to generation of spontaneous activity in rabbit sino-atrial node myocytes. *J. Physiol.,* **434,** 23–40.

DIFRANCESCO, D. (1993). Pacemaker mechanisms in cardiac tissue. *Annu. Rev. Physiol.,* **55,** 455–472.

DIFRANCESCO, D., PORCIATTI, F., JANIGRO, D., MACCAFERRI, G. & COHEN, I.S. (1991). Block of the cardiac pacemaker current ($I_f$) in rabbit sino-atrial node and calf Purkinje fibres by 9-amino-1,2,3,4-tetrahydroacridine. *Pflügers Arch.,* **417,** 611–615.

DOERR, T. & TRAUTWEIN, W. (1990). On the mechanism of the 'specific bradycardic action' of the verapamil derivative UL-FS 49. *Naunyn Schmiedebergs Arch. Pharmacol.,* **341,** 331–340.

FRISHMAN, W.H., PEPINE, C.J., WEISS, R.J. & BAIKER, W.M. (1995). Addition of zatebradine, a direct sinus node inhibitor, provides no greater exercise tolerance benefit in patients with angina taking extended-release nifedipine: results of a multicenter, randomized, double-blind, placebo-controlled, parallel-group study. *J. Am. Coll. Cardiol.,* **26,** 305–312.

GOETHALS, M., RAES, A. & VAN BOGAERT, P.P. (1993). Use-dependent block of the pacemaker current $I_f$ in rabbit sino-atrial node cells by zatebradine (UL-FS 49): On the mode of action of sinus node inhibitors. *Circulation,* **88,** 2389 – 2401.

HARRIS, N.C., LIBRI, V. & CONSTANTI, A. (1994). Selective blockade of the hyperpolarization-activated cationic current ($I_h$ in guinea-pig substantia nigra pars compacta neurones by a novel bradycardic agent, Zeneca ZM 227189. *Neuroscience Letters,* **176,** 221 – 225.

HERMANS, A.N. (1997). Ion translocation by the $Na^+/K^+$ pump: influence of membrane potential and cardiac glycosides. Phd Thesis (Kortrijk). Belgium: Edt. Leuven University Press.

HILLE, B. (1992). *Ionic channels of excitable membranes*. Massachusetts: Sinauer Associates Inc.

HONDEGHEM, L.M. & KATZUNG, B.G. (1977). Time- and voltage-dependent interaction of antiarrhythmic drugs with cardiac sodium channels. *Bioch. Biophys. Acta,* **472,** 373 – 398.

HUGUENARD, J.R. & MCCORMICK, D.A. (1992). Simulation of the currents involved in rhythmic oscillations in thalamic relay neurons. *J. Neurophysiol.,* **68,** 1373 – 1383.

ISENBERG, G. (1976). Cardiac Purkinje fibres: Cesium as a tool to block inward rectifying currents. *Pflügers Arch.,* **365,** 99 – 106.

KAMONDI, A. & REINER, P.B. (1991). Hyperpolarization-activated inward current in histaminergic tuberomammillary neurons of the rat hypothalamus. *J. Neurophysiol.,* **66,** 1902 – 1911.

KOBINGER, W. (1989). Specific bradycardic agents. In *Handbook of experimental pharmacology*, Vaughan Williams, E.M. & Campbell, T.J. (eds.). Vol. **89**. Berlin Heidelberg: Springer Verlag.

KOBINGER, W. & LILLIE, C. (1987). Specific bradycardic agents: a novel pharmacological class? *Eur. Heart J.,* **8** (suppl. L), 7 – 15.

MACCAFERRI, G. & MCBAIN, C.J. (1996). The hyperpolarization-activated current ($I_h$) and its contribution to pacemaker activity in rat CA1 hippocampal stratum oriens-alveus interneurones. *J. Physiol.,* **497(1),** 119 – 130.

MCCORMICK, D.A. & PAPE, H.C. (1990). Noradrenergic and serotonergic modulation of a hyperpolarization-activated cation current in thalamic relay neurones. *J. Physiol.,* **431,** 319 – 342.

MCCORMICK, D.A. & HUGUENARD, J.R. (1992). A model of the electrophysiological properties of thalamocortical relay neurons. *J. Neurophysiol.,* **68,** 1384 – 1400.

NEHER, E. (1992). Correction for the liquid junction potentials in patch clamp experiments. In *Methods in Enzymology*. Bernardo, R. & Iverson, L.E. (eds.). Vol. **207**. San Diego: Academic Press, Inc.

PAPE, H.C. (1994). Specific bradycardic agents block the hyperpolarization-activated cation current in central neurons. *Neuroscience,* **59,** 363 – 373.

PAPE, H.C. (1996). Queer current and pacemaker: the hyperpolarization-activated cation current in neurons. *Annu. Rev. Physiol.,* **58,** 299 – 327.

PERKINS K.L. & WONG, R.K.S. (1995). Intracellular QX-314 blocks the hyperpolarization-activated inward current $I_q$ in hippocampal CA1 pyramidal cells. *J. Neurophysiol.,* **73,** 911 – 915.

PIRCHIO, M., TURNER, J.P., WILLIAMS, S.R., ASPRODINI, E. & CRUNELLI, V. (1997). Postnatal development of membrane properties and $\delta$ oscillations in thalamocortical neurons of the cat dorsal lateral geniculate nucleus. *J. Neurosci.,* **17(14),** 5428 – 5444.

RAES, A., GOETHALS, M., SNOECK, J. & VAN BOGAERT, P.P. (1993). The 'sinus node inhibitor' DK-AH 269 has little effect on the L-type calcium current. *PACE,* **5(II), 1119,** 76.

RAES, A. & VAN BOGAERT, P.P. (1996). Blockade of $I_h$ by the 'sinus node inhibitor' DK-AH 269. *Pflügers Archiv.,* **431(3),** 14.

RAES, A., WANG, Z., VAN DEN BERG R.J., GOETHALS, M., VAN DE VIJVER, G. & VAN BOGAERT, P.P. (1997). Effect of cAMP and ATP on the hyperpolarization-activated current in mouse dorsal root ganglion neurons. *Pflügers Arch.,* **434(5),** 543 – 550.

RANSOM, B.R., NEALE, E., HENKART, M., BULLOCK, P.N. & NELSON, P.G. (1997). Mouse spinal cord in cell culture. I. Morphology and intrinsic neuronal electrophysiologic properties. *J. Neurophysiol.,* **40(5),** 1132 – 1150.

SCROGGS, R.S., TODOROVIC, S.M., ANDERSON, E.G. & FOX, A.P. (1994). Variation in $I_h$, $I_{IR}$, and $I_{LEAK}$ between acutely isolated adult rat dorsal root ganglion neurons of different size. *J. Neurophysiol.,* **71(1),** 271 – 279.

SNYDERS, D.J. & VAN BOGAERT, P.P. (1987). Alinidine modifies the pacemaker current in sheep Purkinje fibers. *Pflügers Arch.,* **410,** 83 – 91.

SOLOMON, J.S. & NERBONNE, J.M. (1993). Hyperpolarization-activated currents in isolated superior colliculus-projecting neurons from rat visual cortex. *J. Physiol.,* **462,** 393 – 420.

STARMER, C.F. (1986). Theoretical characterization of ion channel blockade: ligand binding to periodically accessible receptors. *J. Theor. Biol.,* **119,** 235 – 249.

STERNLICHT, J.P. & VASSALLE, M. (1995). Cesium, $Na^+$-$K^+$ pump and pacemaker potential in cardiac Purkinje fibers. *J. Biomed. Sci.,* **2,** 366 – 378.

THOMAS, R.C. (1972). Intracellular sodium activity and the sodium pump in snail neurones. *J. Physiol.,* **220,** 55 – 71.

TOKIMASA, T., SUGIYAMA, K., AKASU, T. & MUTEKI, T. (1990). Volatile anaesthetics inhibit a cyclic AMP-dependent sodium-potassium current in cultured sensory neurones of bullfrog. *Br. J. Pharmacol.,* **101,** 190 – 192.

TRAVAGLI, R.A. & GILLIS, R.A. (1994). Hyperpolarization-activated currents, $I_H$ and $I_{KIR}$, in rat dorsal motor nucleus of the vagus neurons in vitro. *J. Neurophysiol.,* **71,** 1308 – 1317.

TYTGAT, J., VAN BOGAERT, P.P., VEREECKE, J. & CARMELIET, E. (1992). On the mechanism of action of the bradycardic agent UL-FS 49 on ventricular Ca channels. *Pharmacodyn. Therap. (Life Sci. Adv.),* **9,** 19 – 27.

VALENZUELA C., DELPÓN, E., FRANQUEZA, L., GAY, P., PÉREZ, O., TAMARGO, J. & SNYDERS, D. (1996). Class III antiarrhytmic effects of zatebradine: Time-, state-, use- and voltage-dependent block of hKv1.5 channels. *Circulation,* **94,** 562 – 570.

VAN BOGAERT, P.P. & GOETHALS, M. (1992). Blockade of the pacemaker current by intracellular application of UL-FS 49 and UL-AH 99 in sheep cardiac Purkinje fibers. *Eur. J. Pharmacol.,* **229,** 55 – 62.

VAN BOGAERT, P.P., GOETHALS, M. & SIMOENS, C. (1990). Use- and frequency-dependent blockade by UL-FS 49 of the $I_f$ pacemaker current in sheep cardiac Purkinje fibres. *Eur. J. Pharmacol.,* **187,** 241 – 256.

VAN BOGAERT, P.P. & RAES, A. (1991). Use-dependent blockade of the $I_f$ current by DK-AH 3 in sheep purkinje fibres: kinetic characteristics. *Arch. Intern. Pharmacod.,* **310,** P191.

VAN BOGAERT, P.P. & RAES, A. (1993). Stereoselective use-dependent blockade of the $I_f$ pacemaker current in sheep cardiac Purkinje fibres. *Biophys. J.,* **64(2,2),** A208.

WANG, Z., VAN DEN BERG, R.J. & YPEY, D.L. (1997). Hyperpolarization-activated currents in the growth cone and soma of neonatal rat dorsal root ganglion neurons in culture. *J. Neurophysiol.,* **78,** 177 – 186.

WOLLMUTH, L.P. & HILLE, B. (1992). Ionic selectivity of $I_h$ channels of rod photoreceptors in tiger salamanders. *J. Gen. Physiol.,* **100,** 749 – 765.

*(Received June 17, 1998*
*Revised July 31, 1998*
*Accepted August 5, 1998)*